Exploring Linear and Non-linear AC susceptibilities of Single Crystal Gadolinium around Curie & Spin-reorientation transitions

A Thesis

submitted to
Indian Institute of Science Education and Research Pune
in partial fulfillment of the requirements for the
BS-MS Dual Degree Programme

by

Ananth Kamath

Indian Institute of Science Education and Research Pune
Dr. Homi Bhabha Road,
Pashan, Pune 411008, INDIA.

December, 2022

Supervisor: Dr. Ashna Bajpai

Certificate

This is to certify that this dissertation entitled Exploring Linear and Non-linear AC susceptibilities of Single Crystal Gadolinium around Curie & Spin-reorientation transitions towards the partial fulfilment of the BS-MS dual degree programme at the Indian Institute of Science Education and Research, Pune represents study/work carried out by Ananth Kamath at Indian Institute of Science Education and Research under the supervision of Dr. Ashna Bajpai, Associate Professor, Department of Physics , during the academic year 2022-2023.

Dr. Ashna Bajpai

Committee:

Dr. Ashna Bajpai

Dr. Sunil Nair

This thesis is dedicated to my Father, Mother and Advaith

Declaration

I hereby declare that the matter embodied in the report entitled Exploring Linear and Non-linear AC susceptibilities of Single Crystal Gadolinium around Curie & Spin-reorientation transitions are the results of the work carried out by me at the Department of Physics, Indian Institute of Science Education and Research, Pune, under the supervision of Dr. Ashna Bajpai and the same has not been submitted elsewhere for any other degree.

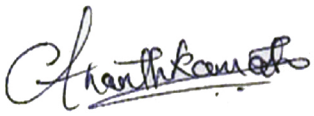

Ananth Kamath

Acknowledgments

I would like to convey my sincerest thanks to my supervisor, Dr.Ashna Bajpai, for her continued expert guidance and constant support. Her strong faith in me motivated me to push through difficult times during the course of this project, professionally and personally. I am eternally grateful to her for providing me with the opportunity to learn and work under her counsel. I am extremely grateful to my TAC member Dr.Sunil Nair for his expert advice and for providing access to his lab facilities

I would like to convey special thanks to my colleague Shashwat Singh Tomar, who helped me immensely with my experiments during the one month I could not walk due to my fractured leg. I would like to express my deepest gratitude to Shruti Chakravarty for her immense help in automating the experimental setup. I am thankful to my labmates Sayan, Ajad and Bharath for their help. I am grateful to my friends Sidharth Adithyan P B, Yogeshraj Nambisan and Vimal Das E S for making the past one year joyous and memorable

Abstract

The aim of this project is to probe the characteristic magnetic properties of elemental gadolinium using the technique of AC magnetic susceptibility. To this end, a home made AC susceptometer was used to probe a polycrystalline and a single crystal gadolinium sample, in the temperature range of 100K to 300K. The first and third order susceptibility of these samples were measured so as to understand the behaviour of gadolinium in the vicinity of two critical transitions: the spin reorientation transition and the Curie transition. To the best of our knowledge, 3rd harmonic susceptibility around these transitions is yet not reported, especially in single crystal samples. While both the samples show a subtle feature around T_{SR} in the first harmonic susceptibility, a sharp feature in the form of cross over around T_C is detected in the third harmonic. Interestingly, previous studies have shown that the sign of the cross-over is reversed in polycrystalline Gd, which we also observe. However the 3rd harmonic susceptibility in the single crystal reveals a new feature, just above the T_C, in addition to the cross-over phenomenon. The 3rd harmonic susceptibility exhibits much sharper transition in the vicinity of the spin-reorientation transition in both polycrystalline and single crystal Gd as compared to what is observed in first harmonic susceptibility . Our data brings forward the importance of higher harmonic susceptibility in exploring complex ferromanet such as Gd, in which interest is rekindled due to a recent report about the possibility of topological magnons.

Contents

List of Tables

List of Figures

Chapter 1

Introduction

This project aims to characterise the magnetic behaviour of Gadolinium metal by exploring it through AC Magnetic Susceptibility. Gadolinium is an elemental ferromagnet, similar to Fe, Co and Ni. It belongs to the rare earth lanthanides series in periodic table, with T_C near the room temperature. It is well known for its magnetocaloric effect and a spin reorientation transition below its ferromagnetic transition T_C. Despite having an easily accessible critical region, a long standing controversy pertaining to gadolinium has been whether Gd is a ferromagnet or a helical antiferromagnet. Though microscopic measurements such as neutron diffraction have confirmed the ferromagnetic phase, the nature of magnetic susceptibility, especially in the critical region were not conclusive. This was primarily due to the existence of twin boundaries in the single crystal and demagnetization field related factors. Recently, the interest in gadolinium has also been rekindled due to the possibility of topological magnons through neutron diffraction measurements[5].

Though, it is relatively easy to explore the critical region, as compared to $3d$ transition metals such as Fe ($T_C \approx 1000$ K) or Ni ($T_C \approx 600$ K), the magnetic state of gadolinium near its T_C and below has not been explored in terms of non linear ac susceptibility, especially in a single crystal sample. For this purpose, a "home-built" AC Susceptometer is used. Depending on the type of magnetic material used, the curves obtained from the temperature sweep of susceptibility will be different. A brief walk-through of relevant terms and properties is presented in the following section.

1.1 Magnetic Materials

Magnetism in solids is a collective phenomenon arising due to: the orbital motion of electrons and the quantum mechanical spin moment and how these electrons are filled in an atom. There are stringent rules to fill the shells. Broadly, materials can be classified into various categories, as will be explored in the following subsections.

1.1.1 Diamagnetic materials

In diamagnetic materials, an applied magnetic field induces a magnetic moment such that it opposes this applied field. Diamagnetism is a weak magnetic phenomenon shown by atoms having no net magnetic moments. This holds even for atoms which have their shells completely filled. In response to an external field (H), by Lenz's law, the current is induced in this system such that it opposes this external field. This induced magnetic moment is proportional to H and the square of the radius at which the electron orbits the nucleus. [2] [6]

1.1.2 Paramagnetic materials

Paramagnetism is shown by materials in which atoms already have a net magnetic moment, due to the presence of unpaired electrons. These moments are not coupled and the thermal energy causes them to be randomly oriented [6]. These moments will line up along the direction of an external applied magnetic field [2]. While an increase in the magnetic field will increase the tendency of spins to line up, an increase in temperature will cause them to randomise. Hence the ratio of the field to temperature will play a big role in the magnetisation of the material. [2]

The evolution of magnetic susceptibility with respect to temperature for paramagnetic materials is described by the Curie law [6]:

$$\chi = \frac{C}{T} \tag{1.1}$$

where, C is the Curie constant (which takes a different values for different materials), T is the temperature of the material.

1.1.3 Ferromagnetic materials

Ferromagnetic materials are the class of magnetic materials which show spontaneous ordering even in the absence of an applied external magnetic field. Unlike the paramagnetic case the spins are able line up in a uniform direction, due to coupling between them. This coupling is generalised as exchange interactions, which originates from electrostatic interactions between electrons and the Pauli exclusion principle[6].

Exchange interactions are electrostatic interactions, arising because charges of the same sign cost energy when they are close together and save energy when they are apart.[2]. If two electrons in an atom have antiparallel spins, then they are allowed to share the same atomic or molecular orbital. However, this will also increase the Coulombic repulsion between the electrons. Hence it is energetically favorable for the electrons to have parallel spin and as a consequence of Pauli's exclusion principle, reside in different orbitals[6]. The Hamiltonian for exchange interactions in ferromagnets is given by

$$H = -\sum_{i,j} J_{ij}\mathbf{S}_i \cdot \mathbf{S}_j \tag{1.2}$$

Here J_{ij} is the exchange integral. It is the term which incorporates the strength of coupling between the two moments i and j. For ferromagnets, the exchange integral is always positive.

The evolution of magnetic susceptibility with respect to temperature for ferromagnetic materials above their Curie temperature is described by the Curie-Weiss law[6]:

$$\chi = \frac{C}{T - \theta} \tag{1.3}$$

where, C is the Curie constant (which takes a different values for different materials), T is the temperature of the material. Here, θ is related to molecular field proposed by Weiss. When it is positive, elementary magnetic moments are aligned in parallel direction. When T = θ , there is a divergence in the susceptibility, indicating a phase transition to the ferromagnetic phase.

1.1.4 Antiferromagnetic materials

When the exchange interaction **J** is negative, it is favorable for the adjacent spins to align in an antiparallel fashion. In the bulk, this will result in a net magnetic moment of zero. Antiferromagnetism is typically modeled using Weiss theory [6]. In the Weiss model, the molecular field is divided into two sub-lattices. The magnetic moments point in opposite directions in either sub-lattices.

The Curie-Weiss law followed by antiferromagnets above their Neel transition temperature is given by

$$\chi = \frac{C}{T + \theta} \tag{1.4}$$

For antiferromagnets , theta is negative. This signifies a negative molecular field , that favors anti parallel alignment of the moments. This temperature is known as Neel temperature (T_N). The spontaneous magnetisation of antiferromagnets is zero below T_N. However, practically, they do show a finite, but very small magnetization [7].

Another mechanism in which antiferromagnetism arises can be explained through RKKY interaction. In rare earth metals, the separation between magnetic ions is too large to have any coupling between them. In this case, an ion polarises conduction electrons surrounding it. Since electrons are delocalised in such a system, this polarisation is transferred to other magnetic ions, thus propogating the polarisation. This is known as the Ruderman–Kittel–Kasuya–Yosida interaction (referred to as RKKY interaction in short) [6]. However, depending on the distance between the ions, this interaction can result in positive or negative **J**. In the cases in which the distance is such that the **J** is negative, we observe antiferromagnetism.

1.1.5 Helical Ordering

Helical ordering or helical antiferromagnetism is a special case of magnetic ordering found in rare-earth metals like dysprosium. In these elements, the crystal structure is such that the atoms are arranged in layers (the majority having hexagonal close packed structure) [2]. In the case where there is ferromagnetic alignment of moments within a layer, the interaction between these layers can be described by two exchange interaction constants J_1 and J_2 for nearest-neighbour and next-nearest-neighbour interactions respectively. Now, if the angle

between the consecutive basal planes is θ, then the energy of the system can be written as [2]

$$E = -2NS^2(J_1 \cos\theta + J_2 \cos 2\theta) \tag{1.5}$$

For getting the states with energy minima, we take the partial derivative of the above equation and equate it to zero ($\partial E/\partial\theta = 0$). We get

$$(J_1 + 4J_2 \cos\theta)\sin\theta = 0 \tag{1.6}$$

There are three solutions to this equation: $\theta = 0$ (ferromagnetic case), $\theta = \pi$ (antiferromagnetic case) and

$$\cos\theta = \frac{-J_1}{4J_2} \tag{1.7}$$

This solution will be preferred over ferromagnetic and antiferromagnetic cases when $J_2 < 0$ and $|J_1| < 4|J_2|$ [2]. Generally, the pitch of the spiral wont be commensurate with the lattice parameter, so no two layers in the crystal will have the exact same spin direction [2].

In summary, a schematic for various types of magnetic ordering which has been discussed in previous sections is presented in Figure 1.1

1.2 Gadolinium

Gadolinium is considered to be one of the four ferromagnetic elements alongside Iron, Cobalt and Nickel. It exhibits a ferromagnet to a paramagnet transition at 293K [8]. Another magnetic transition shown by gadolinium is the spin reorientation transition, at 230K which is associated with the change in the easy axis of magnetization [8]. Gadolinium is also one of the rare materials that exhibit the magnetocaloric effect. Gadolinium is widely regarded as a ferromagnet. Gadolinium is a reactive metal: it forms gadolinium oxide when exposed to moist air.

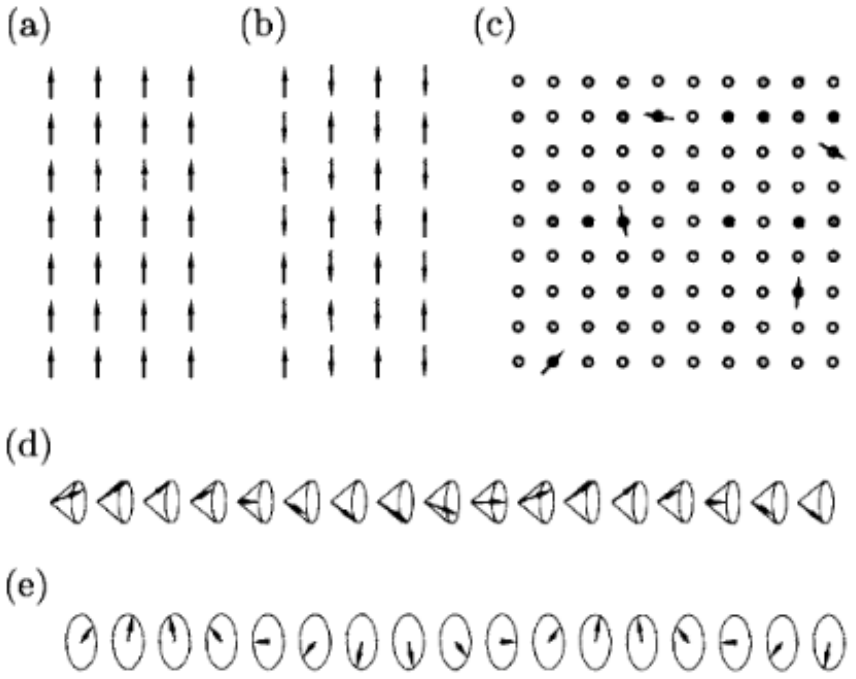

Figure 1.1: Various types of Magnetic Order: (a)Ferromagnetic order, (b)Antiferromagnetic order, (c)Spin Glass, (d)Spiral order, (e)Helical order. Image taken from source[2]

1.2.1 Curie Transition of Gadolinium

The paramagnet to ferromagnet transition is a second order phase transition. Second order phase transitions occur when a new state of reduced symmetry develops at a lower temperature, resulting in an ordered phase. This is a continuous transition from the disordered (high temperature) paramagnetic phase. Second order phase transition is indicated are also characterized by divergent susceptibility, infinite correlation length, and power law decay of correlations near criticality. Gadolinium shows such a transition from a ferromagnet to paramagnet at 293K[8].

1.2.2 Spin Reorientation Transition

Ferromagnetic and antiferromagnetic materials often show a preferred axis of magnetisation, called the "easy-axis" of magnetisation. This easy axis coincides with crystallographic di-

rections of high symmetry. This magnetic anisotropy is caused by two factors: short range spin-orbit coupling and long range dipole interactions. In some materials this easy axis of magnetisation changes its direction at a certain temperature. This is called the spin reorientation transition and the temperature at which it occurs is known as the spin reorientation temperature T_{SR}.

For gadolinium, this temperature is around 230K[8]. The easy axis of gadolinium coincides with the six-fold symmetry axis: the C-axis. In gadolinium, the direction of magnetic moments is parallel to this hexagonal C-axis from T_C to T_{SR}[8]. Below T_{SR}, the moments tilts away from the C-axis till a maximum of 60 degrees (at around 180K), after which they tilt back to under 30 degrees at lower temperatures[8].

1.2.3 Magnetocaloric Effect

Magnetocaloric effect (or Adiabatic demagnetisation as it is alternatively known as) refers to the phenomenon of the temperature of certain materials changing on exposure to magnetic fields. Gadolinium is one such material in which this effect is pronounced. All magnetic materials show the magnetocaloric effect, but the strength of the effect varies between materials. This effect originates from the coupling of the magnetic sublattice with the externally applied magnetic field, changes the magnetic contribution of entropy to the solid[3].

The magnetocaloric effect can be compared to the thermodynamics of gases: isothermal compression, where we apply pressure, resulting in the entropy of the gas decreasing is similar to isothermal magnetisation. In isothermal magnetisation, we apply a magnetic field to reduce the magnetic entropy of the system[3]. Similarly, adiabatic expansion of a gas is equivalent to adiabatic demagnetisation: the external magnetic field is removed, but the entropy remains constant, as a result we get a reduction in temperature of the sample[3].

1.2.4 Is Gadolinium a conventional or complex ferromagnet?

Even though gadolinium is widely accepted to be an elemental ferromagnet, there has been considerable debate surrounding this, one very popular proposition being that it is a helical antiferromagnet[9]. The debate was initiated by Belov and Pedko, by observing the peculiar

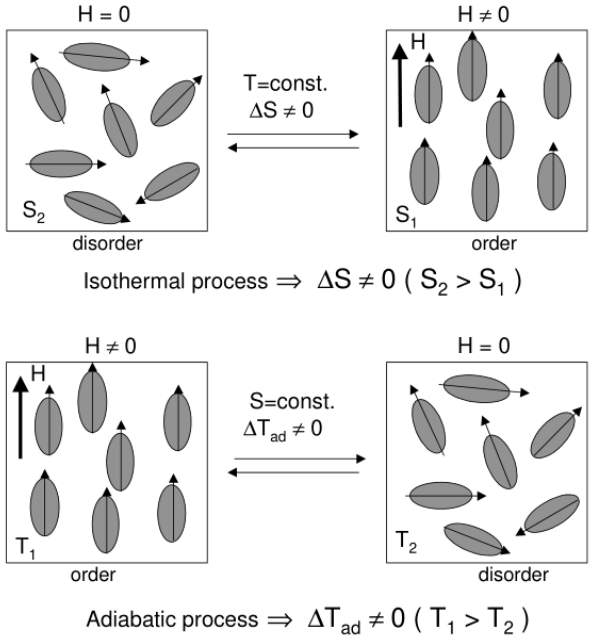

Figure 1.2: Graphic explaining Isothermal Magnetisation and Adiabatic Demagnetization. H is the applied magnetic field, T is the temperature and S is the entropy. (image taken from source[3])

patterns in the thermomagnetic response of a polycrystalline Gd sample at low magnetic fields ($\leq$15 Oe) between 210K and 293K (the T_C), concluded that gadolinium has a helical spin structure (a special antiferromagnetic order)[10]. The resultant curves and kinks that they found were similar to those of Dysprosium at critical fields that mark the disappearance of helical magnetism[10]. They claimed that the reason helical antiferromagnetism was not observed normally is because even weak fields could destroy the antiferromagnetic ordering. It is important here to note that these observations were performed on polycrystalline toroidal gadolinium samples, which already introduces a structural anisotropy. Later magnetic investigations[11], including neutron diffraction experiments[12][13] on single crystal gadolinium showed no patterns of helical antiferromagnetism. While Gd is established to be a ferromagnet, it appears to be a complex ferromagnet. This is concluded from various anomalies in magnetization near the critical region.

1.3 Magnetic Susceptibility

Magnetic Susceptibility describes the magnetic nature of a given material and the degree to which it responds to an external field. It is calculated using the magnetisation M and applied magnetic field H. Magnetisation is defined as the total magnetic moment per unit volume. This total magnetic moment is the added-up result of magnetic contributions from the atomic level[14].

Magnetic susceptibility of a material is defined as the ratio of its magnetisation M to the induced magnetic field H in the limit of H tending to zero:

$$\chi = \lim_{h \to 0} \frac{M}{H} \tag{1.8}$$

Oftentimes, the magnetic susceptibility is also defined as differential susceptibility,

$$\chi = \frac{\partial M}{\partial H} \tag{1.9}$$

We can get a better insight into a particular material's magnetic properties by applying a sinusoidally varying magnetic field, $H = H_{dc} + H_{ac} \cos \omega t$, with $\omega = 2\pi f$ being the frequency of the field. The susceptibility measured under such a magnetic field is what is known as AC Magnetic Susceptibility. Assuming the system gives a linear response, it is defined as

$$\chi_{ac} = \frac{M_{ac}}{H_{ac}} \tag{1.10}$$

However, most systems, including gadolinium, give off a much layered non-linear response in reaction to a varying magnetic field. In such cases, the magnetisation M can be polynomially expanded as a function of H [15] [14]

$$M = M_0 + \chi_1 H + \chi_2 H^2 + \chi_3 H^3 + \dots \tag{1.11}$$

where χ_1 is the linear susceptibility and M_0 is the spontaneous magnetisation casued by internal field. Quite often, only the odd powers of H are required in the above expansion. This changes in cases where an internal symmetry breaking field may be present, in which case χ_2 can be observed[14].

The magnetisation by itself is a function of time and can be written as[14]:

$$M = M_0 + m\cos(\omega t - \theta) \tag{1.12}$$

As AC susceptibility χ_{ac} is actually complex valued quantity, it can split into real and imaginary parts: $\chi_{ac} = \chi^r + i\chi^i$, in which χ^r is the component in phase with the applied AC field and χ^i is the out of phase component. Using this, one can obtain $\chi^r = m\cos\theta/H_{ac}$ and $\chi^i = m\sin\theta/H_{ac}$. Applying these to susceptibilities of all order and applying fourier expansion, the following expression is obtained[16] [17] [14]:

$$M = M_0 + H_{ac}\sum_{n=1}^{\infty}(\chi_n^r\cos(n\omega t) + \chi_n^i\sin(n\omega t)) \tag{1.13}$$

where χ_n^r and χ_n^i are the in phase and out of phase component of the n^th order susceptibility. From the above equation, it can be seen that the susceptibility of order n can be observed by simply going to $n\omega$. Depending on how large the frequency ω is in comparison to the response time τ of the system, we can probe various regimes of the system. The aforementioned description of AC susceptibility is valid in the intermediate regime, where $\omega \approx 1/\tau$. When $\omega >> 1/\tau$, the adiabatic susceptibility of the system is measured, whereas when $\omega << 1/\tau$, the isothermal susceptibility is obtained[18] [14].

1.3.1 Standard linear and nonlinear susceptibility responses of various magnetic materials to temperature

This work deals with measurement of nonlinear susceptibility in the elemental ferromagnet, gadolinium. In this subsection, we describe the general features of nonlinear susceptibility in various magnetic phases. Our main focus would be on the transitions exhibited by ferromagnetic and antiferromagnetic materials. The characteristic temperature dependent curves are shown in Figure 1.3.

Paramagnetic substances show a simple inverse relation to temperature as described by the Curie law. In ferromagnets, the first order susceptibility χ_1 diverges at T_C. The χ_2 as well as χ_3 show a similar pattern in that they both shoot up in magnitude and show a change in sign at T_C. Antiferromagnets have their χ_1 increasing in magnitude at T_N and then reducing back down again, approaching zero. They exhibit no 2^{nd} order susceptibility. The

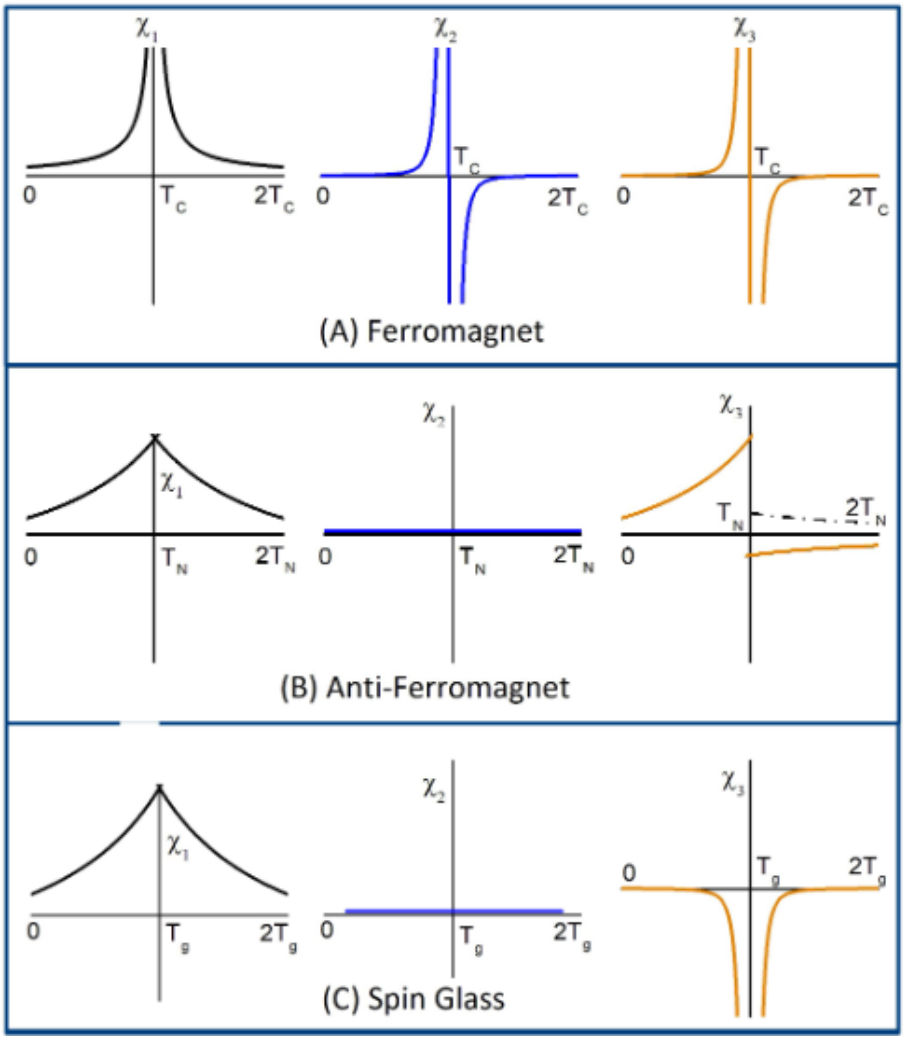

Figure 1.3: Responses of various types of magnetic materials to AC χ (image taken from reference[4]

χ_3 signature is interesting in that it does show a discontinuous a change in signal magnitude near T_C. But depending on the coordination number, the value it falls to can be negative or positive, hence the crossover transition is dependent on the internal symmetry of the sample[19].

Spin glasses are characterised by the inherent randomness of their spins and the cooperative property of these spins, which causes them to freeze at a particular temperature[16]. It is a disordered state when compared to ferromagnets, the couplings are too random in spin glass systems. Their signature under AC χ is the negative divergence of χ_3 at the transition temperature[20]. It is interesting to note that a cross over in sign is expected in χ_3 in the

vicinity of T_C, with χ_3 being negative above T_C. These predictions are based on Landau theory of phase transition. However polycrstalline Gd samples have shown an reverse behaviour near T_C. Also these studies were not extended to spin reorientation region. To the best of our knowledge there is no higher harmonic studies in single crystal.

1.4 AC Magnetic Susceptometer

A "home-made" AC Susceptometer was used for measuring both linear and non linear susceptibilities in both polycrystalline and single crystal samples of Gd. . The setup involves a few key components: a temperature controller, a Lock-in Amplifier (LIA), a set of primary and secondary coils, double evacuated quartz tubes, a sample rod which will be inserted into the inner evacuated quartz tube and a glass Dewar to hold the cryogen (liquid nitrogen) in which the quartz tube will be dipped for cooling.

The setup contains two coaxial quartz tubes, with the facility to evacuate the interspace region between both the quartz tubes as well as the inner quartz tube, which forms the sample chamber. The inner tube acts as the sample chamber. A gate valve is present on top of these tubes, through which the sample rod can be inserted in the sample chamber through a Wilson seal.

The primary and secondary coils are setup such that the secondary sits concentrically inside the primary. The secondary coil set consists of two coils, wound in series opposition. The quartz tubes sits concentrically inside both the primary and secondary. The primary coil generates the AC magnetic field when AC current is passed through this coil. This magnetic field induces magnetization in the sample, which is kept in one of the secondaries.

The Sample rod is made using a hollow metallic rod, below which a cylindrical hylam section is attached. At the end of this hylam section, the sapphire plates which act as the sample holder is attached. As the sample holder, two sapphire plates are attached in an overlapping way, vertically, using GE Varnish. A heater coil (phosphor-bronze wire in our case) is wound over these sapphire plates, ensuring that it does not encroach too much into the second sapphire plate which will hold the sample. At the very edge of the second sapphire plate, the sample is glued and wound with teflon tape to ensure it stays in place. Above the sample, but below the heater coil, on the second sapphire plate, the Platinum Resistance

Thermometer (PRT), which allows us to measure the temperature of the sample, is attached.

Both coils and the quartz tube are dipped in the cryogen filled glass Dewar. This ensures that throughout the experiment, both the coils are at a uniform temperature. The sample temperature is decided by the interplay of a few factors: resistance of the heater coil, the current passed through the heater coil, presence of exchange gas (Helium) in inner as well as interspace. The exchange gas may be introduced into the inner and interspace to facilitate the initial cooling of the sample to the boiling point of liquid nitrogen (77K), after which it is removed from the inner space. A constant pressure of helium is left in the interspace. The parameters of the temperature controller is set taking into account this pressure and the resistance of the heater coil, so that the heating process is smooth, allowing the sample to reach and stabilise at the required temperature within a reasonable time frame.

The Susceptometer setup was automated by visual coding using LabView software, for which the required drivers for Stanford Research model SR830 Lock-in Amplifier and LakeShore 336 Temperature Controller were procured and used within the software.

Chapter 2

Calibration of AC-Susceptibility bridge

This chapter is about calibration of AC Susceptibility bridge using standard paramagnetic salts such as Gd_2O3 and Er_2O3. Here we measure first harmonic susceptibility as a function of temperature and determine C and θ from Curie-Weiss law.

2.1 Modifications to the Susceptometer

Before calibration the existing (homemade) AC Susceptibility setup was de-assembled. Due to repeated thermal cycling, the coil set needed a fresh coat of GE Varnish followed by baking. In addition to this in the sample holder, the existing PRT had to be replaced due to magnetic impurity. The Manganin heater wire is slightly magnetic, while it was a sufficient distance away from the sample holder, a safer route of replacing it with the non-magnetic Phosphor-Bronze heater wire. Since Phosphor-Bronze is a low resistivity alloy, a larger length had to be wound. Consequently, the Sample Holder design had to be changed from the single Sapphire plate to two single-crystal sapphire plates attached on either flat sides of a polycrystalline sapphire plate. This design change was done to ensure better stability and thermal contact of the sample holder.

Subsequently a dry run of temperature against 1^{st}, 2^{nd} and 3^{rd} order susceptibilities with

Figure 2.1: New Sample Holder

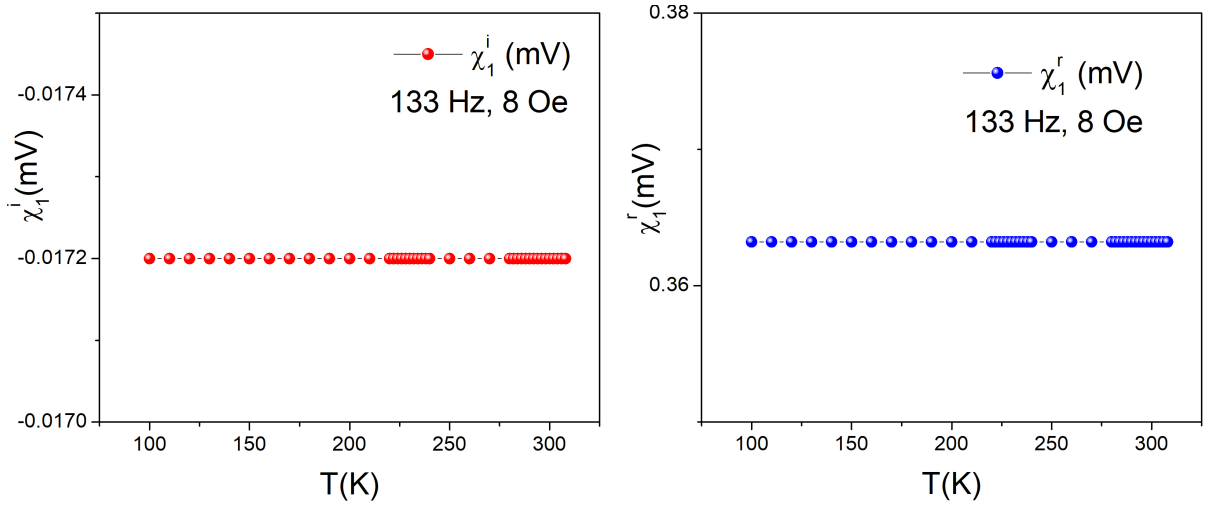

Figure 2.2: Dry Run data: χ_1^i on the left with a constant value of -0.0172 mV and χ_1^r on the right with a constant value of 0.3632 mV

the new sample holder on the sample rod was taken. In the dry run, the sample rod is inserted into the setup without any sample on the sample holder, while subjecting it to the same value of field and frequency as we would to a sample (in this particular case, we apply 8 Oe field at 133Hz). This is done to register the signal values given off by the sample rod and these values will be subtracted from the data taken during sample runs. The graphs of the dry run are shown in Figures 2.2, 2.3 and 2.4

As the graphs show, the 1^{st} harmonic shows a constant background while the higher harmonics are negligibly small. In this particular run, the offset in 3rd harmonic is small, but changes of the order of 1 to 2 μV are observed. Hence it is crucial to take dry run,

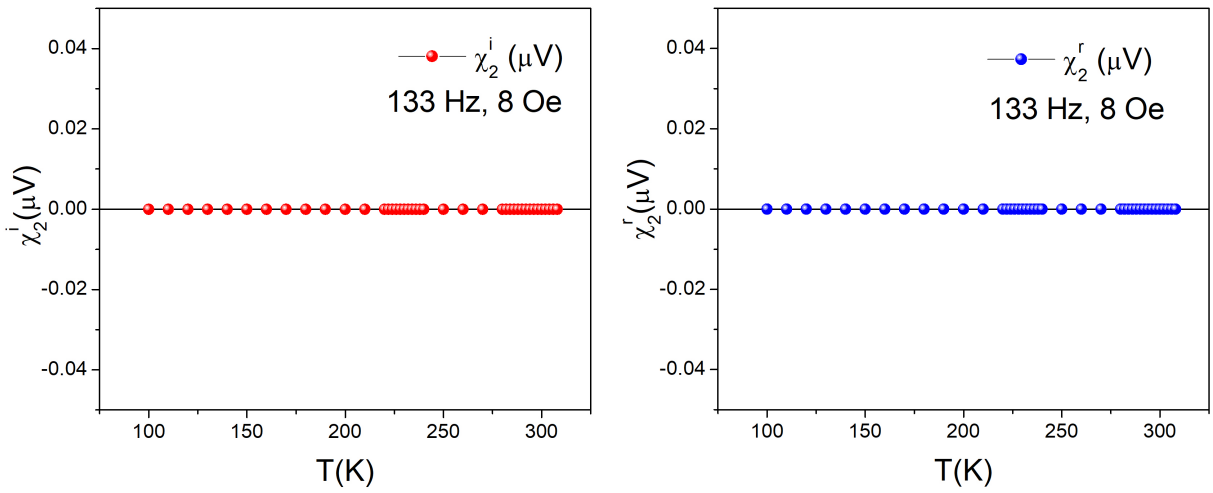

Figure 2.3: Dry Run data: χ_2^i on the left χ_2^r on the right, both are 0 μV

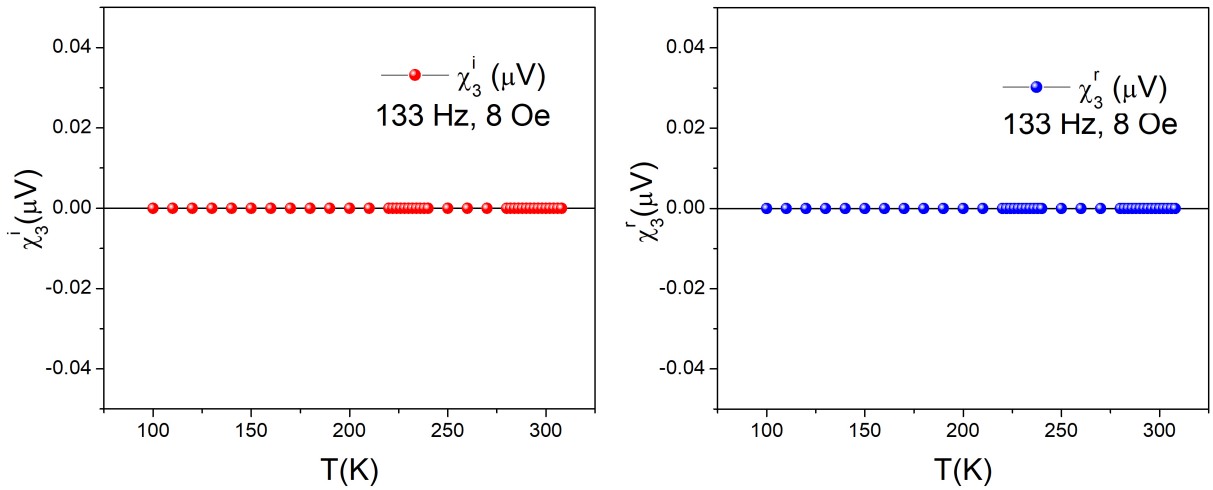

Figure 2.4: Dry Run data: χ_2^i on the left χ_2^r on the right, both are 0 μV

especially when the 3rd harmonic signal is small.

2.2 Calibration of the Susceptometer

The Susceptometer was calibrated using the standard paramagnetic samples of Gd_2O_3 and Er_2O_3, procured from Sigma-Aldrich, both of 99.9 % purity . The samples, which were in powdered form, were pelletized using a KBR-press. The obtained Gd_2O_3 and Er_2O_3 pellets were of masses 345.3 mg and 76.9 mg respectively. In our case, the equation relating the

	C ($cm^3 K mol^{-1}$)		θ (K)	
Sample	Fitted	Literature	Fitted	Literature
Gd_2O_3	8.6	8.3	-27.1	-18.4
Er_2O_3	10.6	11.1	-10.4	-13.4

Table 2.1: Comparison table of Curie-Weiss parameter values obtained from experiment and existing literature values[1]

signal voltage value from the Lock-in Amplifier to the Susceptibility goes as[21]

$$v = \frac{M \cdot f \cdot H \cdot \chi}{\alpha} \tag{2.1}$$

where v is the signal voltage, α is the calibration constant, M is the number of moles of the paramagnetic salt used, f is the frequency of the applied field, H is the value of the applied field and χ is the susceptibility according to Curie-Weiss law.

As part of the calibration procedure, the real part of the first order susceptibility, ${\chi_1}^r$, of both Gd_2O_3 and Er_2O_3 was plotted against temperature. The $\frac{1}{{\chi_1}^r}$ was fitted linearly against temperature. Throughout both temperature sweeps, both the 2^{nd} and 3^{rd} harmonics were measured to be zero. Using the obtained slope and intercept, the samples were calibrated both ways: i.e, the Gd_2O_3 sample was calibrated using the Er_2O_3 curve and vice-versa. The intercept θ and the obtained slope, which is the Curie constant C is tabulated and compared to the respective literature values in 2.1[1] [22].

The graphs of the ${\chi^r}_1$ both Gd_2O_3 and Er_2O_3 has been plotted and is shown in Figures 2.5 and 2.6. In both sets of graphs, there is a visible deviation from standard paramagnetic behavior above 250 K. We can conclude that this is due to some systematic error. Hence the fitting was done upto 245K for both paramagnetic salts. Er_2O_3 usually gives much lesser signal than Gd_2O_3, combined with the factor of the Er_2O_3 pellet weighing around only one-third of the Gd_2O_3 pellet, the difference in signal magnitude is large, therefore another run with a bigger sample mass would help to better calibrate the instrument.

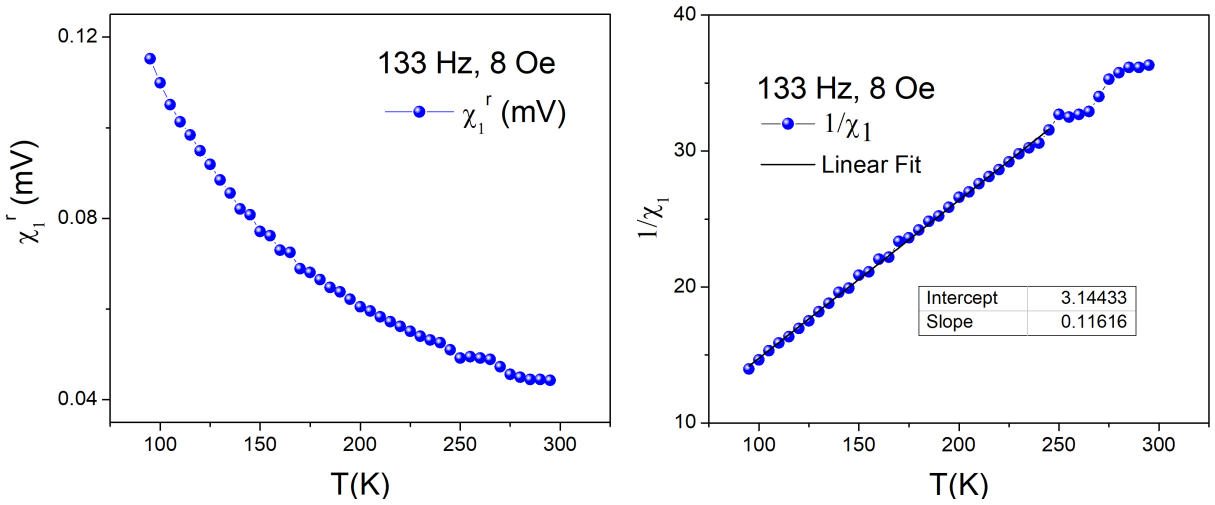

Figure 2.5: Gd_2O_3 calibration data: Offset corrected χ_1^r data on the left; $\frac{1}{\chi}$ curve calibrated and linear fitted using α of Gd_2O_3 the right

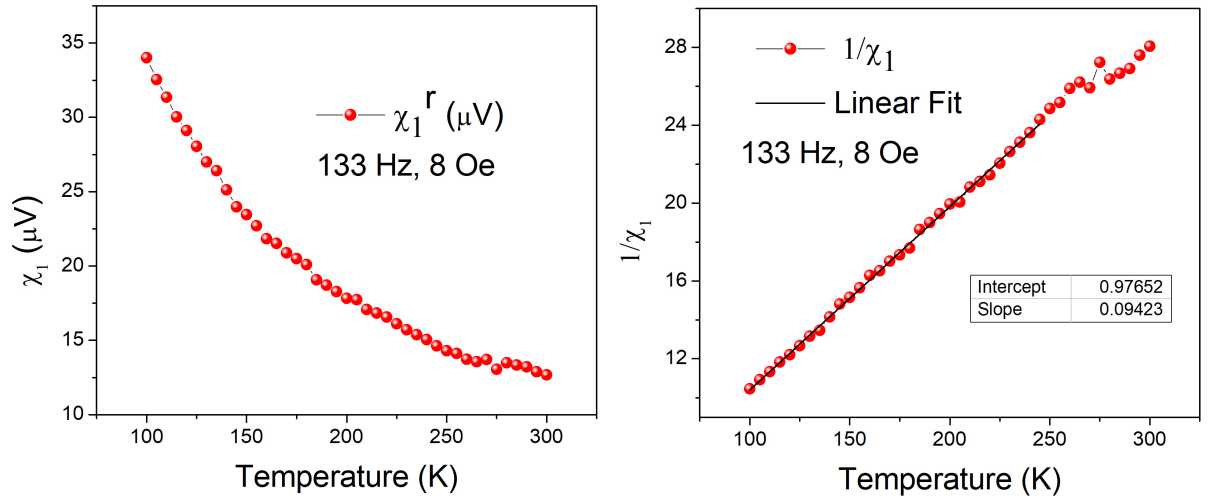

Figure 2.6: Er_2O_3 calibration data: Offset corrected χ_1^r data on the left; $\frac{1}{\chi}$ curve calibrated and linear fitted using α of Gd_2O_3 the right

Chapter 3

Probing Gd using AC Susceptibility

In order to extract as much information about the magnetic behaviour of Gadolinium metal, the AC Susceptibility technique was applied on both polycrystalline and single crystal Gadolinium samples.

3.1 Polycrystalline Gadolinium sample

A 73.3 mg sample of polycrystalline Gd sample was used for the experiment. A temperature sweep of the 1^{st} and 3^{rd} harmonics were performed manually from 100K to 308K. The sample was subjected to 8 Oe field and 133 Hz frequency in this run. During the experiment, data was taken at an interval of 10K from 100K to 240K and 240K to 280K. The increment was 2K in the range of 220K to 240K and 280K to 308K. This was done in hopes of locating the two key transitions of gadolinium: the Spin reorientation transitions and Curie transition. The data for the first and third order susceptibilities are shown in figures 3.1 and 3.2.

From the χ_1^r data, we can see that there is a change in slope of signal values from 220K to 290K. This is consistent with the susceptibility data obtained on Gd single crystal, when measurements are conducted in the crystallographic direction perpendicular to C axis[8]. However the polycrystalline sample, with randomly oriented grains, also shows similar feature, though it is smeared off, as is expected for a polycrystal. The spin re-orientation transition in the vicinity of 230K is also associated with another slope change, which is very

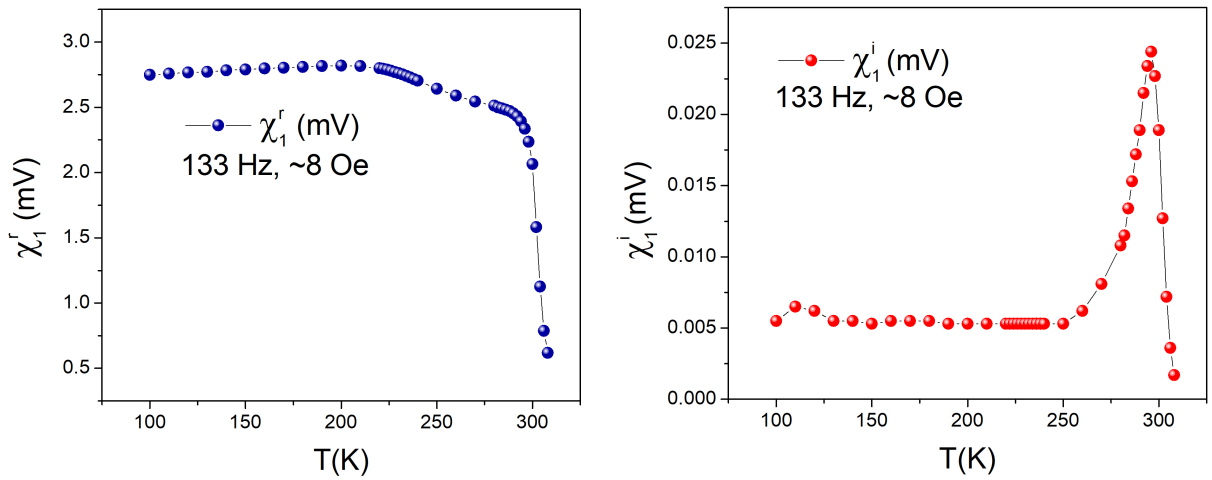

Figure 3.1: Polycrystalline Gadolinium Data: χ_1^r on the left and χ_1^i on the right

mild. After 290K, the dropoff becomes steeper, indicating the Curie transition process. χ_1^i also shows a peak like effect in the vicinity of Curie transition. However no major changes are detected neat the spin re orientation transition.

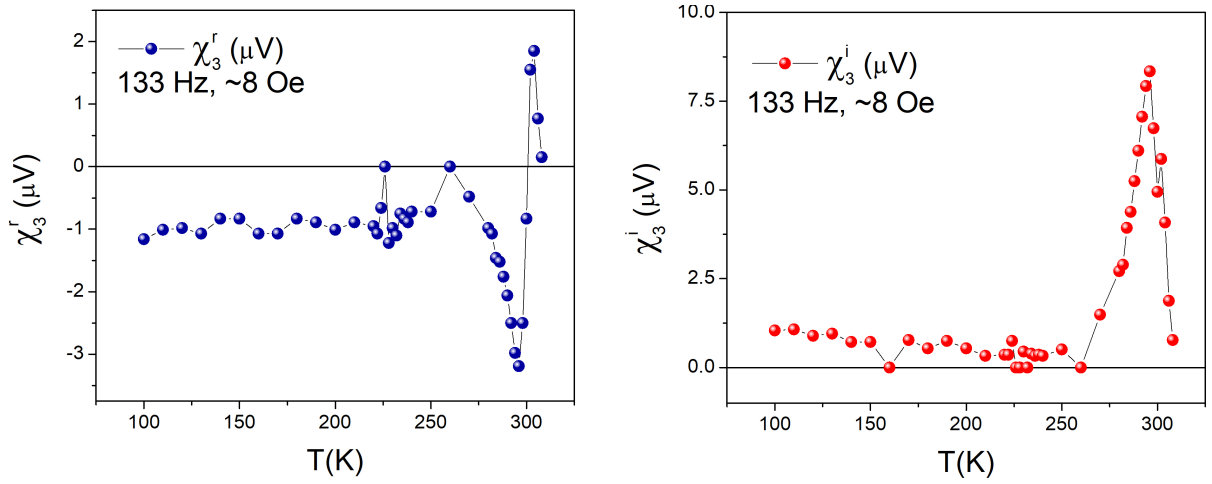

Figure 3.2: Polycrystalline Gadolinium Data: χ_3^r on the left and χ_3^i on the right

The χ_3 plots shows a sharp anomaly around the Curie transition and also shows a change of sign. However, this change of sign is just opposite to what is predicted for a routine ferromagnet. This anomalous behaviour is already reported for polycrystalline Gd [23]. The χ_3 around T_{SR} also shows features, which are sharper as compared to what is seen in χ_1^r. However more data points are needed in the vicinity of T_{SR}.

3.2 Single-Crystal Gadolinium sample

The Gadolinium single-crystal sample used for the experiment weighed 235.5mg (obtained from Professor Tamizhavel, TIFR). AC-χ measurements were conducted perpendicular to the C-axis, at two field values of 4.8 Oe and 8 Oe, both at a frequency of 133 Hz. The temperature sweep was taken from 100K to 319K, presented in Figure 3.3. Closer data points were taken in the vicinity of T_C as well as T_{SR}.

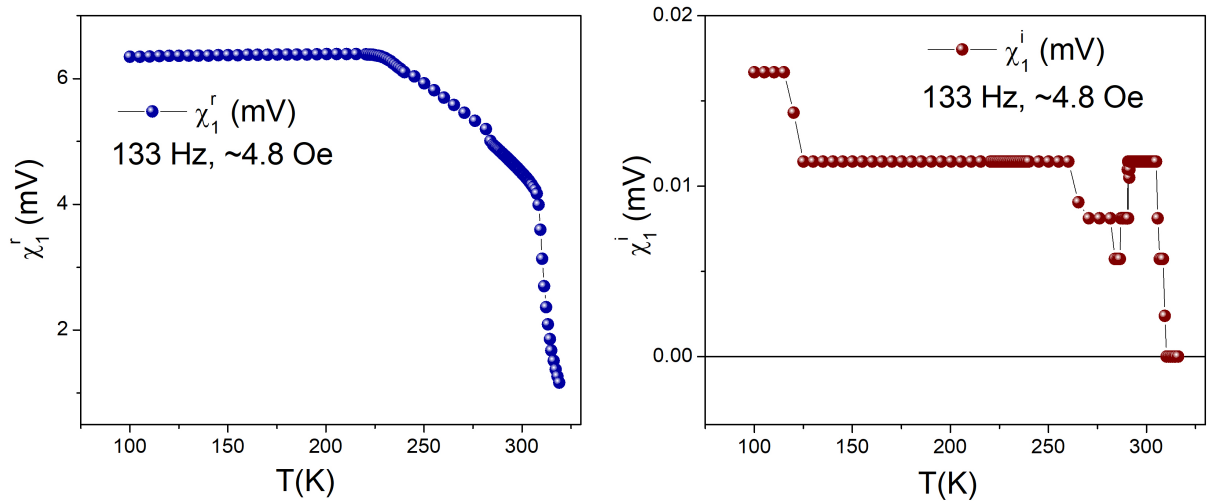

Figure 3.3: Single-Crystal Gadolinium Data, taken under a field of 4.8 Oe: χ_1^r on the left and χ_1^i on the right.

The χ_1^r data is again consistent with previous reports[8]. The change around T_C is much sharper as compared to what is seen around T_{SR}. In case of the single crystal, the imaginary part (χ_1^i) is much smaller in magnitude as compared to χ_1^r when data is taken at 4.8 Oe. Thus accurate offset data is needed to isolate signal from background.

The χ_3 plots show a rich signature near the transition region. Three clear peaks can be seen in χ_3^r and two peaks in χ_3^i (see insets of both graphs in Figure 3.4). As is evident from Figure 3.4 (a) and 3.4 (b), a sharp change is observed in both χ_3^r and χ_3^i in the vicinity of

χ_1^r/χ_1^i	χ_3^r/χ_3^i
115	0.22

Table 3.1: Comparison table of signal magnitude ratios for polycrystalline Gadolinium sample. Ratios obtained from the value of the highest positive peaks.

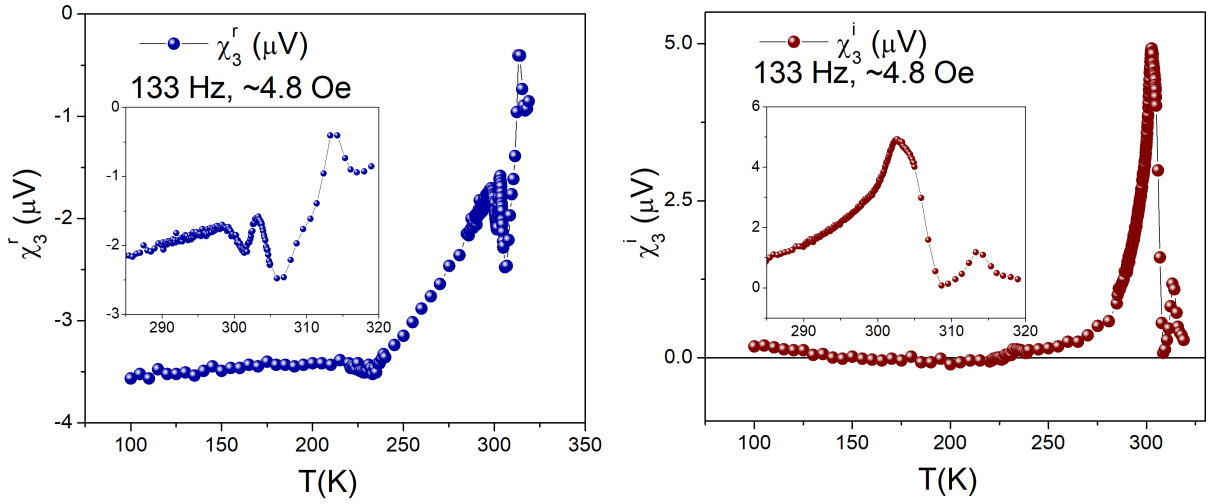

Figure 3.4: Single-Crystal Gadolinium Data, taken under a field of 4.8 Oe: χ_3^r on the left (inset: 285K to 305K of the same curve) and χ_3^i on the right (inset: 285K to 305K of the same curve).

T_C and T_{SR}. Just above the T_C, an additional feature is observed in both the real and the imaginary part, the origin of which is unknown at this point. Whether this feature is intrinsic, needs further investigation. It is interesting to note that χ_3^r shows a sharp change near T_C, though it remains negative through out and does not show cross over phenomenon. Similar features have been earlier reported in polycrystalline Gd. To the best of our knowledge, there is no χ_3 data on a single crystal, similar to what we present here.

The 8 Oe, 133 Hz run is plotted in Figures 3.5 and 3.6. The χ_1^r is identical to the 4.8 Oe run, though χ_1^i is better resolved in higher H, exhibiting a peak like behaviour near T_C. No major changes are detected near T_{SR}. The χ_1^i shows a clear local maxima at 300.2K. The χ_3^r, shows sharp anomaly near the T_C and a very well resolved dip near the T_{SR}. Thus it is clear that both the transitions, especially subtle transition like T_{SR} are better resolved using higher harmonic susceptibility. Also additional feature near the T_C, which was observed in 4.8 Oe is also present in 8 Oe data. These additional features are highlighted in the inset in Figures 3.4 and 3.5.

Field (Oe)	χ_1^r/χ_1^i	χ_3^r/χ_3^i
4.8	376	0.39
8	641	0.29

Table 3.2: Comparison table of signal magnitude ratios for Single-Crystal Gadolinium sample. Ratios were obtained from the value of the highest positive peaks

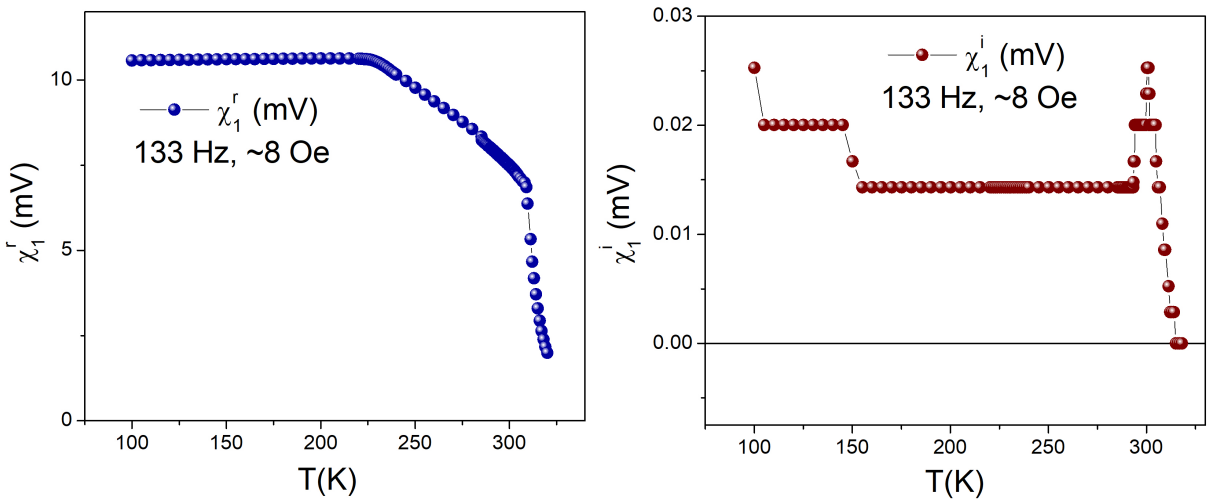

Figure 3.5: Single-Crystal Gadolinium Data, taken under a field of 8 Oe: χ_1^r on the left and χ_1^i on the right.

In order to understand the field dependence of the 1^{st} and 3^{rd} order susceptibilities, field-normalised comparison plots were made.

Field normalized data for χ_1 and χ_3 is presented in Figures 3.7 and 3.8 respectively. While no major field dependence is reported for χ_1^r , χ_1^i shows a slight field dependence and the magnitude of χ_1^i is larger for larger H. A significant field dependence is seen in in χ_3 data in the vicinity of T_C as well as T_{SR}.

Typically a change of sign is expected in the vicinity of T_C for a routine ferromagnet [23]. It is expected to be negative above T_C and positive below T_C. However in case of poly-crystalline gadolinium , an opposite trend was seen, which was highly field dependent. This was explained by taking into account domain wall dynamics. Our data on single crystal Gd, which also reports a new feature just above T_C further confirms that Gd is a complex ferromagnet and more field and frequency dependent runs, along different crystallographic directions are needed to understand this elemental fetromagnet.

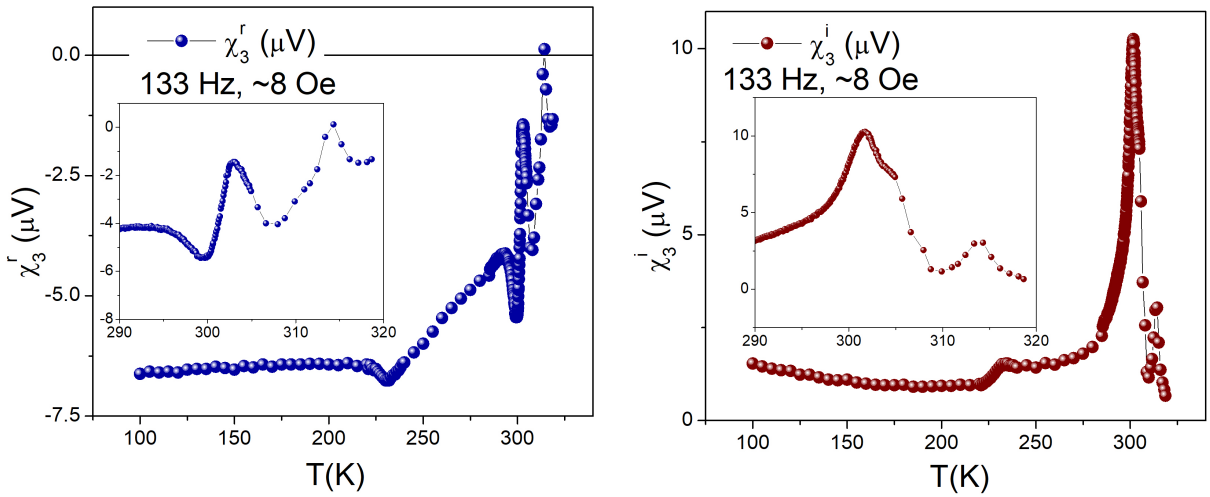

Figure 3.6: Single-Crystal Gadolinium Data, taken under a field of 8 Oe: χ_3^r on the left and χ_3^i on the right

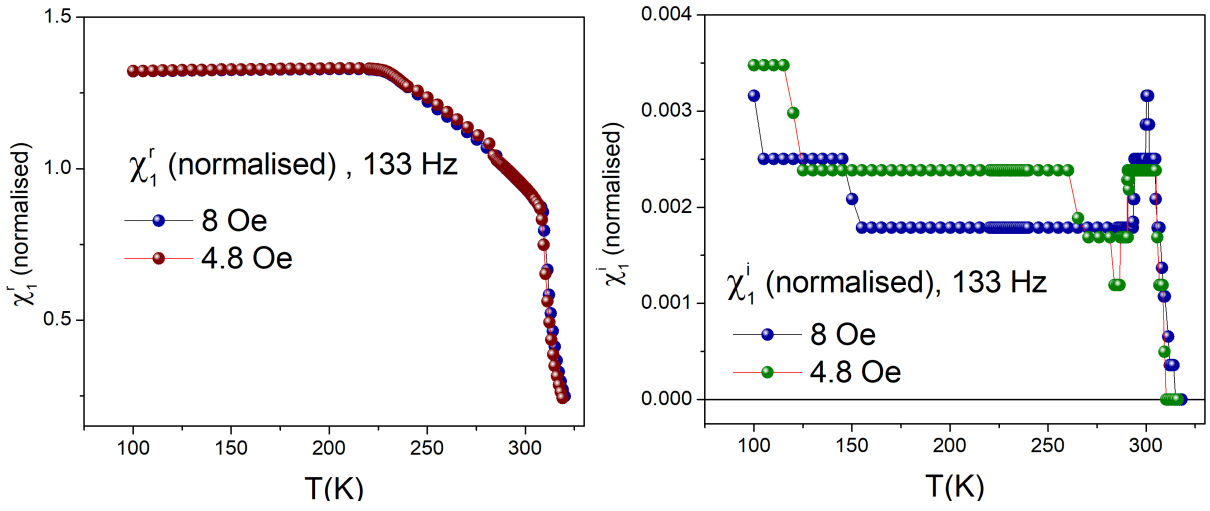

Figure 3.7: Field normalised χ_1^r (left) and χ_1^i (right) comparison plot

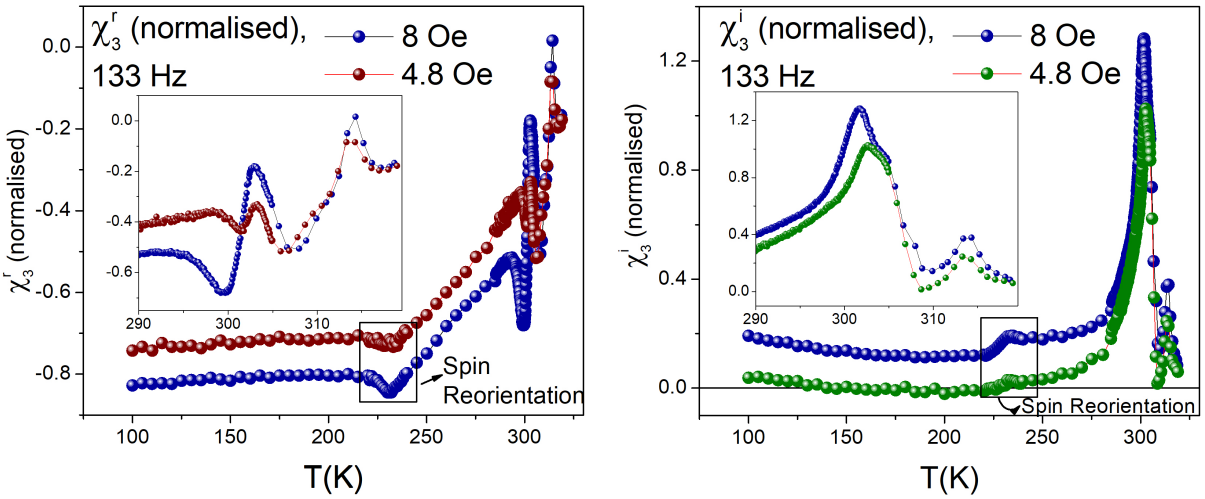

Figure 3.8: Field peak normalised χ_3^r (left) and χ_3^i (right) comparison plots

3.3 Comparison between Gd samples

Figure 3.9 (a) and 3.9 (b) show comparison of χ_1^r and χ_1^i between the single crystal and the polycrystalline sample used in this study. The transition is sharper in the single crystal in χ_1^r near T_C , but the loss part is better resolved in the polycrystalline sample. This can also be understood from the point of view of domain wall motion. There are likely to be more pinning centers in a polycrystalline sample, leading to a well resolved χ_1^i, as shown in Figures 3.9 and 3.10.

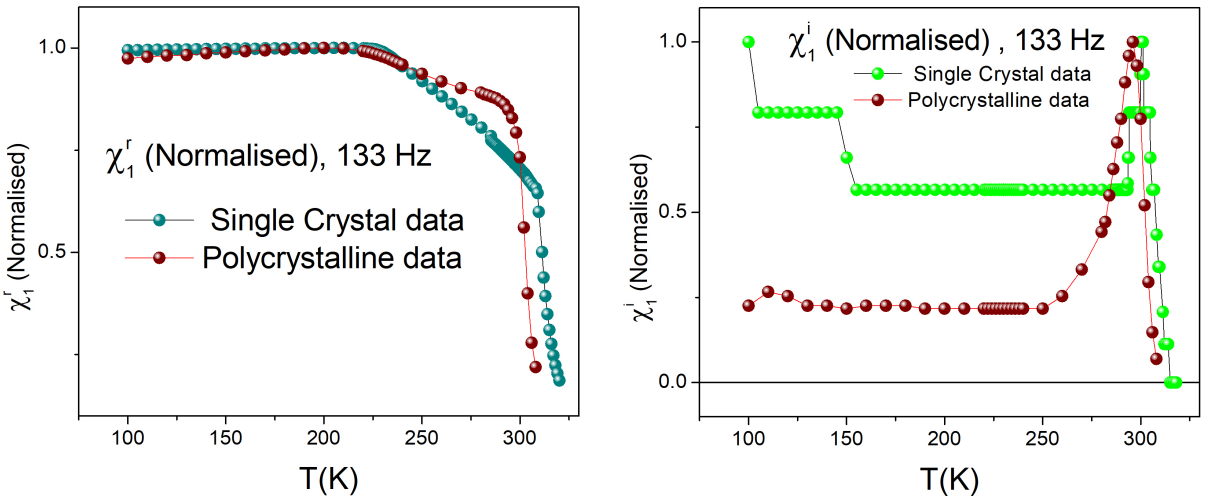

Figure 3.9: Peak signal normalised χ_1^r (left) and χ_1^i (right) comparison plots

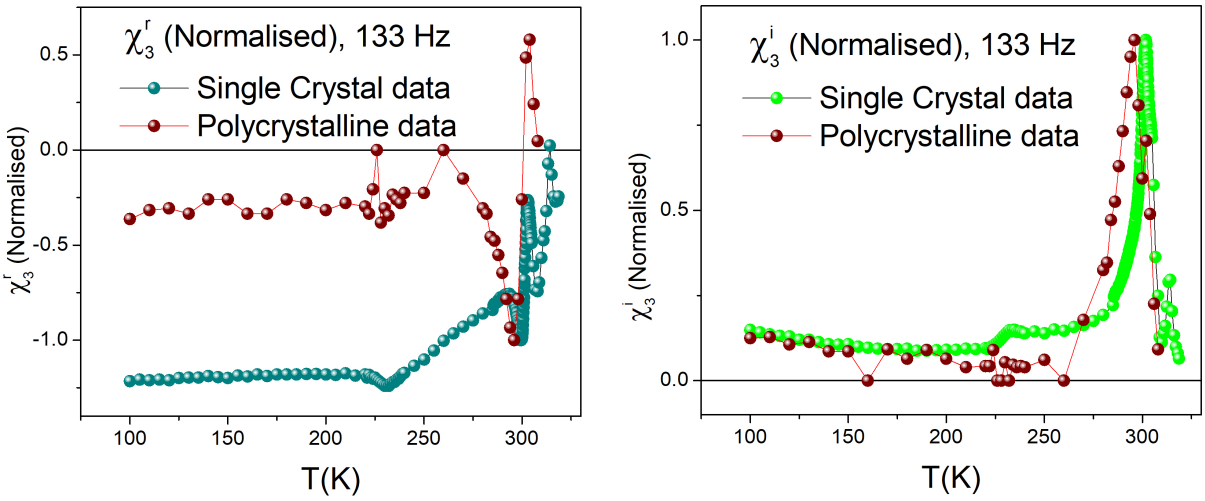

Figure 3.10: Peak signal normalised χ_3^r (left) and χ_3^i (right) comparison plots

The normalised χ_3^r plots presented in this work are normalised with their lowest respective local minima in the range of 290K to 320K. It is also interesting to note that χ_3^r in the polycrystalline sample does show the change of sign, which is opposite to theoretical expectations. This anomalous behaviour is reported for polycrystalline Gd [23] .This feature is explained by modification on Landau theory of phase transitions. While our data on polycrystalline sample is similar to previous observations, the data on single crystal shows sharp changes around T_C, as well as an additional feature just above T_C. Since this is probably the first report on χ_3 in Gd single crystal, the origin of this new features is still unclear. It is yet to be ascertained whether this feature is intrinsic or extrinsic. However overall, the high resolution χ_3 data as presented here, clearly indicate that subtle features such as T_{SR} and complexity involved around a magnetic transition are better resolved in higher harmonics susceptibility.

Chapter 4

Conclusion and Further work

We have presented linear and non linear susceptibilities of both polycrystalline as well as single crystal Gd in the vicinity of the Curie as well as spin reorientation transition. Our data shows that both the transitions are better resolved in higher harmonic susceptibility. The real part of third harmonic susceptibility shows a cross over in sign near T_C, which is reverse of what is expected in a routine ferromagnet. The third harmonic susceptibility in the single crystal sample also shows a sharp change near T_C and a very clear dip around the T_{SR}. In addition, a new feature is observed just above T_C, the origin of which is unknown. More field and frequency runs are needed to understand the critical region in elemental Gd, which offers a very interesting magnetization dynamics around the magnetic transition, as is evident from our linear and non linear susceptibility data. We also need better background correction in both first and the third harmonic, particularly near the room temperature.

Bibliography

[1] S. Arumugam, N. Manivannan, and A. Murugeswari. Simple uniaxial pressure device for ac-susceptibility measurements suitable for closed cycle refrigerator system. *Review of Scientific Instruments*, 78(6):063906, 2007.

[2] S. Blundell. *Magnetism in Condensed Matter*. Oxford Master Series in Condensed Matter Physics. OUP Oxford, 2001.

[3] Fèlix Casanova i Fernàndez. *Magnetocaloric Effect In Gd5(SixGe1-x)4 Alloys*. PhD thesis, 2004.

[4] L. Holleis, J.C. Prestigiacomo, and Z. et al. Fan. Anomalous and anisotropic nonlinear susceptibility in the proximate kitaev magnet alpha-rucl3. *npj Quantum Mater.*, 6, 2021.

[5] A. Scheie, Pontus Laurell, P. A. McClarty, G. E. Granroth, M. B. Stone, R. Moessner, and S. E. Nagler. Dirac magnons, nodal lines, and nodal plane in elemental gadolinium. *Phys. Rev. Lett.*, 128:097201, Mar 2022.

[6] Nicola A. Spaldin. *Magnetic Materials: Fundamentals and Applications*. Cambridge University Press, 2 edition, 2010.

[7] E. Coronado, B. S. Tsukerblat, and R. Georges. *Molecular Magnetism: From Molecular Assemblies to the Devices*, chapter Exchange Interactions I: Mechanisms, pages 65–84. Springer Netherlands, Dordrecht, 1996.

[8] S. N. Kaul and S. Srinath. Gadolinium: A helical antiferromagnet or a collinear ferromagnet. *Phys. Rev. B*, 62:1114–1117, Jul 2000.

[9] J. M. D. Coey, V. Skumryev, and K. Gallagher. Rare-earth metals: Is gadolinium really ferromagnetic? *nat*, 401(6748):35–36, 1999.

[10] K.P. Belov and A.V. Ped'ko. "Helical" Antiferromagnetism of Gadolinium. *Sov. Phys. JETP*, 15:62–64, September 1962.

[11] S. Yu. Dan'kov, A. M. Tishin, V. K. Pecharsky, and K. A. Gschneidner. Magnetic phase transitions and the magnetothermal properties of gadolinium. *Phys. Rev. B*, 57:3478–3490, Feb 1998.

[12] G. Will, R. Nathans, and H. A. Alperin. Neutron diffraction investigation of a gadolinium single crystal. *Journal of Applied Physics*, 35(3):1045–1046, 1964.

[13] J. W. Cable and E. O. Wollan. Neutron diffraction study of the magnetic behavior of gadolinium. *Phys. Rev.*, 165:733–734, Jan 1968.

[14] C V Topping and S J Blundell. A.c. susceptibility as a probe of low-frequency magnetic dynamics. *Journal of Physics: Condensed Matter*, 31(1):013001, nov 2018.

[15] A. Banerjee, A. Bajpai, and Sunil Nair. *Probing Magnetic Phases in Different Systems using Linear and Non Linear Susceptibility*, pages 43–69. Springer Berlin Heidelberg, Berlin, Heidelberg, 2005.

[16] J. A. Mydosh. *Spin glasses : an experimental introduction*. Taylor and Francis, 1993.

[17] T. Ishida and R. B. Goldfarb. Fundamental and harmonic susceptibilities of $yba_2cu_3o_{7-\delta}$. *Phys. Rev. B*, 41:8937–8948, May 1990.

[18] Dante Gatteschi, Roberta Sessoli, and Jacques Villain. *Molecular Nanomagnets*. Oxford University Press, 03 2006.

[19] Sumiyoshi Fujiki and Shigetoshi Katsura. Nonlinear Susceptibility in the Spin Glass. *Progress of Theoretical Physics*, 65(4):1130–1144, 04 1981.

[20] Yoshihito Miyako, Susumu Chikazawa, Toshiaki Saito, and Y. G. Yuochunas. Nonlinear magnetization at the spin glass phase transition temperature. *Journal of the Physical Society of Japan*, 46(6):1951–1952, 1979.

[21] Martin Nikolo. Superconductivity: A guide to alternating current susceptibility measurements and alternating current susceptometer design. *American Journal of Physics*, 63(1):57–65, 1995.

[22] A. Bajpai and A. Banerjee. An automated susceptometer for the measurement of linear and nonlinear magnetic ac susceptibility. *Review of Scientific Instruments*, 68(11):4075–4079, 1997.

[23] Takashi Shirane and Shohei Sakurai. Nonlinear susceptibilities of gadolinium near curie temperature. *Journal of Korean Physical Society*, 62(12):2173–2178, June 2013.